

## Synthesis of zeolite L from natural zeolite by alkaline fusion-hydrothermal treatment Síntesis de zeolita L a partir de zeolita natural mediante tratamiento de fusión alcalina-hidrotermal

M.G. Guerrero-Olvera <sup>a</sup>, F. Legorreta-García <sup>a</sup>, D. Díaz-Guzmán <sup>a</sup>, M. Vargas-Ramírez <sup>a</sup>  
E.A. Chávez-Urbiola <sup>a</sup>, N.K. Pérez-González <sup>a,\*</sup>

<sup>a</sup> Área Académica de Ciencias de la Tierra y Materiales, Universidad Autónoma del Estado de Hidalgo, 42184, Pachuca, Hidalgo, México.

### Abstract

In this work, the synthesis conditions of zeolite L using alkaline fusion-hydrothermal treatment (F-H treatment), as well as its ion exchange capacity, are studied. To obtain zeolite L, natural zeolite, Al(OH)<sub>3</sub> and KOH were mixed in different proportions to obtain two precursor mixtures. Each mixture was calcined at 400 °C for two hours and then the synthesis reaction was carried out in a hydrothermal reactor at 145 °C for 50 and 90 hours. The zeolite obtained was analyzed using X-ray Diffraction, Scanning Electron Microscopy and Inductively Coupled Plasma Mass Spectrometry characterization methods. Ion exchange was carried out at 25 °C for 24 hours, contacting the synthetic zeolites obtained with a 1000 ppm Cu(NO<sub>3</sub>)<sub>2</sub> solution. The ion exchange capacity of Cu<sup>2+</sup> was analyzed using the UV-Vis spectrophotometry method, where it was found that the synthesized zeolites have an exchange capacity of 34.59 mg/g, which is superior to natural zeolite (6.88 mg/g).

**Keywords:** Synthesis, Zeolite L (LTL), alkaline fusion-hydrothermal treatment, natural zeolite, ion exchange.

### Resumen

En este trabajo se estudian las condiciones de síntesis de la zeolita L mediante tratamiento de fusión alcalina-hidrotermal, así como su capacidad de intercambio iónico. Para obtener la zeolita L se mezcló zeolita natural, Al(OH)<sub>3</sub> y KOH a diferentes proporciones para obtener dos mezclas precursoras. Cada mezcla fue calcinada a 400 °C durante dos horas y posteriormente la reacción de síntesis se llevó a cabo en un reactor hidrotermal a 145 °C durante 50 y 90 horas. La zeolita obtenida se analizó mediante los métodos de caracterización de Difracción de Rayos X, Microscopía Electrónica de Barrido y Espectrometría de Masa con Plasma Acoplado Inductivamente. El intercambio iónico se realizó a 25 °C durante 24 horas poniendo en contacto las zeolitas sintéticas obtenidas con una solución de Cu(NO<sub>3</sub>)<sub>2</sub> de 1000 ppm. La capacidad de intercambio iónica de Cu<sup>2+</sup> se analizó mediante el método de espectrofotometría UV-Vis donde se encontró que las zeolitas sintetizadas presentan una capacidad de intercambio de 34.59 mg/g, que es superior a la zeolita natural (6.88 mg/g).

**Palabras Clave:** Síntesis, Zeolita L (LTL), tratamiento de fusión alcalina-hidrotermal, zeolita natural, intercambio iónico.

### 1. Introduction

Zeolites are crystalline aluminosilicate materials characterized by their 3D structure composed of TO<sub>4</sub> tetrahedrons (T=Si, Al), where each oxygen bonds to two T atoms. They also have channels and cavities of molecular sizes that can accommodate cations, water and other molecules (Guth *et al.*, 1999). There are two types of zeolites according to their origin: natural and synthetic. For example, clinoptilolite is a fairly common natural zeolite and L-type

zeolite was first synthesized and patented by Breck and co-workers (Breck *et al.*, 1965).

Zeolite L is identified with the code LTL, according to IUPAC nomenclature. It has been synthesized mainly by the hydrothermal treatment, sometimes using prior aging of the components. The most common precursors are high-purity chemicals such as hydroxides, silicates and silica in solution, which are highly reactive. Typical reaction temperatures reported in the literature are between 150-180 °C, at different

\* Autor para la correspondencia: pe219945@uaeh.edu.mx (Nelly K. Pérez-González)

**Correo electrónico:** gu335985@uaeh.edu.mx (María Guadalupe Guerrero-Olvera), profe\_974@uaeh.edu.mx (Felipe Legorreta-García), lestamian@uaeh.edu.mx (Damián Díaz-Guzmán), marissav@uaeh.edu.mx (Marissa Vargas-Ramírez), chavez.urbiola@gmail.com (Edgar Arturo Chávez-Urbiola)

reaction times (see Table 1). However, to date, the synthesis of zeolite L has not been reported using the alkaline fusion-hydrothermal treatment (F-H treatment) and using zeolite clinoptilolite as silica source. It has been reported that the alkaline fusion method allows the activation of aluminosilicate-rich raw materials -kaolin, fly ash, clays-, obtaining a higher reactivity of the precursors to produce high quality zeolites (Ayele *et al.*, 2016; Kazemian *et al.*, 2010). Moreover, because clinoptilolite is an abundant mineral, it could decrease the cost of reagents and make the synthesis economically viable.

On the other hand, due to the regular shape of its pores and its adsorbent properties, zeolite L has been used to accommodate organic dyes (Gartzia-Rivero *et al.*, 2017). Saepurahman and co-workers used the L-type zeolite to remove methylene blue from wastewater (Saepurahman *et al.*, 2015). Other works report the use of zeolite L to capture

organic dye molecules and create fluorescent materials (Insuwan *et al.*, 2015; Leire *et al.*, 2017). Zeolite L has also been applied in catalysis where it is used as a support for metals such as Pt (Chen *et al.*, 2018). Other researchers have doped zeolite L films with iron nanoparticles to detect CO<sub>2</sub> and O<sub>2</sub> in the gas phase (Georgieva *et al.*, 2017). The performance of these processes will depend on the physical properties of the zeolite, such as crystal size and morphology. For example, disk-shaped zeolite L crystals can be used in photonic devices (Veiga-Gutiérrez *et al.*, 2012).

The purpose of this work is to study the different reaction conditions to synthesize a zeolite L. The synthesis was done by alkaline fusion-hydrothermal treatment, using natural clinoptilolite-type zeolite, KOH and Al(OH)<sub>3</sub>. Finally, the ion exchange capacity of the obtained zeolite and the natural zeolite is compared.

Table 1. Synthesis conditions of zeolite L (LTL).

Synthesis method	Materials	Reaction conditions	References
Hydrothermal treatment	Al(OH) <sub>3</sub> , KOH, silica solution, Ba(NO <sub>3</sub> ) <sub>2</sub>	175 °C for 24 h	Zhao <i>et al.</i> , 2018.
Hydrothermal with the previous aging	NaAlO <sub>2</sub> , KOH, silica solution, NaOH, FeCl <sub>3</sub>	80 °C for 3 days; 180 °C for 1 día	Zhang <i>et al.</i> , 2020.
Hydrothermal treatment	(Al <sub>2</sub> (SO <sub>4</sub> ) <sub>3</sub> 18H <sub>2</sub> O, KOH, silica solution, C <sub>2</sub> H <sub>5</sub> OH (co-solvente).	150-180 °C for 3-7 days	Gomez <i>et al.</i> , 2011.
Hydrothermal with the previous aging	Al <sub>2</sub> (SO <sub>4</sub> ) <sub>3</sub> 18-H <sub>2</sub> O, Al(OH) <sub>3</sub> , silica solution, KOH.	180 °C for 3 days	Lee <i>et al.</i> , 2005.
Hydrothermal treatment	Colloidal silica or fumed silica, aluminum powder, KOH.	160-170 °C for 24 h	Itani <i>et al.</i> , 2011

## 2. Methodology

### 2.1. Zeolite synthesis

Zeolite synthesis was carried out by performing the fusion method followed by hydrothermal treatment, using two precursor mixtures with different proportions of natural zeolite, KOH y Al(OH)<sub>3</sub>, see table 2. Composition by weight (%) of natural zeolite, previously analyzed by x-ray fluorescence (Pérez González, 2019), is SiO<sub>2</sub>=70.02%, Al<sub>2</sub>O<sub>3</sub>=11.05%, K<sub>2</sub>O=3.25%, Fe<sub>2</sub>O<sub>3</sub>=1.48%, CaO=1.78%, MgO=1.45% y H<sub>2</sub>O=10.43%. The general synthesis procedure is described below and is schematized in Figure 1:

1. Natural zeolite with a particle size of 75 µm was mixed with potassium hydroxide (KOH) and aluminum hydroxide (Al(OH)<sub>3</sub>). The amount and total molar composition of the reagents depending on the different mixtures that were used are shown in Table 2.

2. The resulting mixture was homogenized by pulverizing the reagents by using an agate mortar.
3. The precursor powder was placed in a melting pot and calcined to complete the alkaline fusion treatment of the components at a temperature of 400 °C for 2 hours.
4. The resulting pellet was crushed and placed in a Teflon vessel together with 30 ml of deionized water.
5. The synthesis reaction was carried out in a hydrothermal reactor at 145 °C for 50 and 90 hours.
6. The synthesized solid product was washed with deionized water and recovered by centrifugation to subsequently be dried at 100 °C.

Analysis of the liquid product was performed by Inductively Coupled Plasma (ICP) Mass Spectrometry to determine elemental concentrations. The solid product was characterized by X-Ray Diffraction (XRD) and Scanning Electron Microscopy (SEM) techniques.

Table 2: Quantity of reagents for the precursor mixtures.

	Natural Zeolite	KOH	Al(OH) <sub>3</sub>	H <sub>2</sub> O	Molar composition (mmol)
Mixture-1	3	1.12	0.156	30 ml	47.6 SiO <sub>2</sub> : 3.3 Al <sub>2</sub> O <sub>3</sub> : 1.04 K <sub>2</sub> O: 0.28 Fe <sub>2</sub> O <sub>3</sub> : 0.95 CaO: 1.08 MgO: 17.37 H <sub>2</sub> O: 2 Al(OH) <sub>3</sub> : 20 KOH: 1665 H <sub>2</sub> O
Mixture-2	12	4.4815	0.624	30 ml	190.4 SiO <sub>2</sub> : 13.2 Al <sub>2</sub> O <sub>3</sub> : 4.16 K <sub>2</sub> O: 1.12 Fe <sub>2</sub> O <sub>3</sub> : 3.8 CaO: 4.32 MgO: 69.48 H <sub>2</sub> O: 8 Al(OH) <sub>3</sub> : 80 KOH: 1665 H <sub>2</sub> O

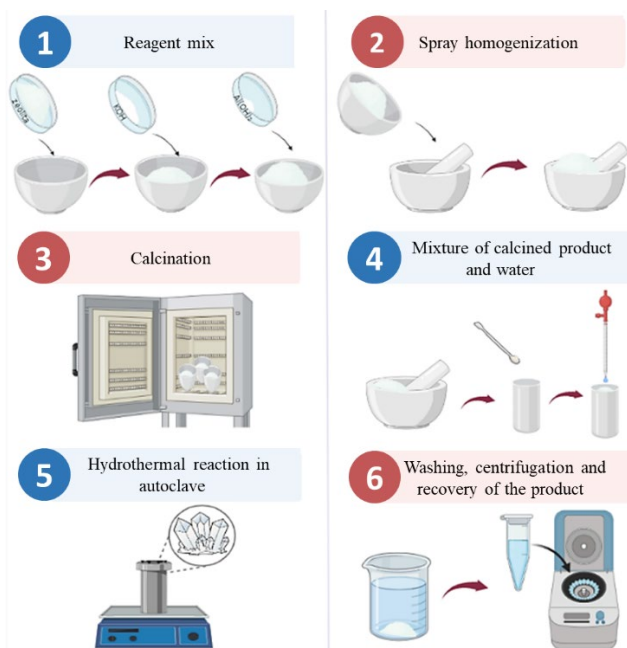


Figure 1. Diagram of the synthesis process of type L zeolite using natural zeolite, KOH and  $\text{Al}(\text{OH})_3$  as precursors by alkaline fusion-hydrothermal (F-H) treatment.

## 2.2. Ion exchange with $\text{Cu}^{2+}$

The ion exchange of the synthesized zeolites and the natural zeolite was initiated by preparing a solution of copper nitrate ( $\text{Cu}(\text{NO}_3)_2 \cdot 3\text{H}_2\text{O}$ ) at 1000 mg/L (ppm) of  $\text{Cu}^{2+}$ . Subsequently, 50 ml of this solution with 0.5 g of zeolite was stirred at a temperature of 25 °C for 24 hours.

## 3. Results and discussion

### 3.1. X-Ray Diffraction Analysis

It was done the XRD analysis on natural zeolite and zeolites synthesized from potassium hydroxide (KOH), aluminum hydroxide ( $\text{Al}(\text{OH})_3$ ) and natural zeolite using the F-H treatment for 50 and 90 hours at 145 °C.

Figure 2-a shows the diffractogram of the natural zeolite composed of clinoptilolite (Gottardi *et al.*, 2013) and opal (Curtis *et al.*, 2019) phases. Figure 2-b shows the zeolite obtained with the F-H treatment using mixture-2 at 145 °C for 50 hours, which corresponds to the type L zeolite reported by Sato and co-workers (Sato *et al.*, 1990). Figure 2-c belonging to the zeolite synthesized for 90 hours, shows a diffraction pattern similar to that of zeolite synthesized for 50 hours, with slight variations in the intensity of some peaks. Similarly, this zeolite obtained was found to be the L type.

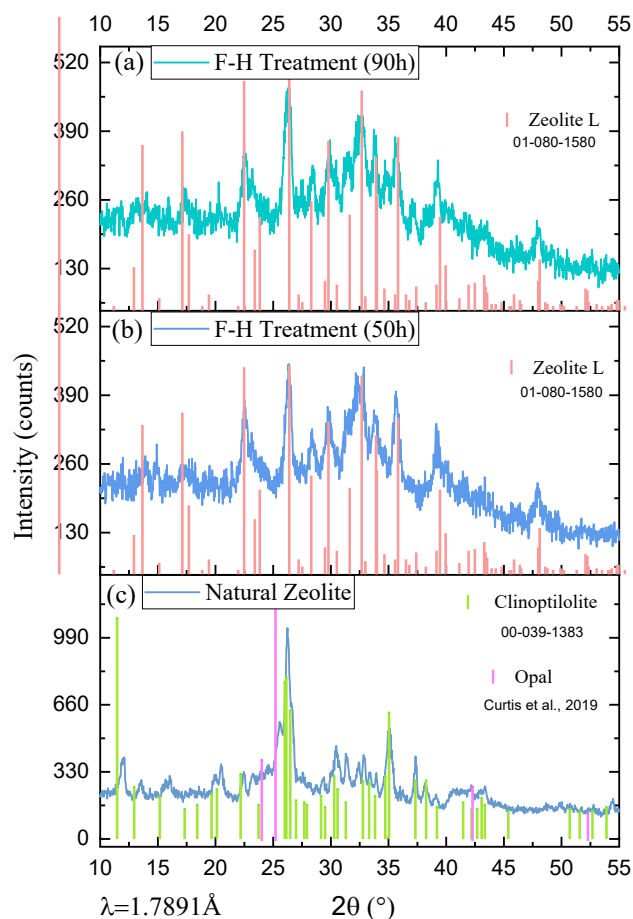


Figure 2. Diffractograms (XRD) were obtained from the zeolites synthesized using mixture-2 as a precursor with reaction times of (a) 90 hours and (b) 50 at 145 °C and (c) natural zeolite. The reference diffraction patterns of clinoptilolite and zeolite L were taken from the ICDD database (PDF-X2/Full File 2004).

Figure 3 shows the crystal structure of zeolite L obtained from the Database of Zeolite Structures (2022), which is composed of silicon, aluminum and oxygen tetrahedrons, as well as exchangeable potassium and sodium cations. This type of zeolite has channels with diameters of 7.1 Å (Barrer *et al.*, 1969), which is greater than the maximum pore diameter of the zeolite clinoptilolite (3.67 Å).

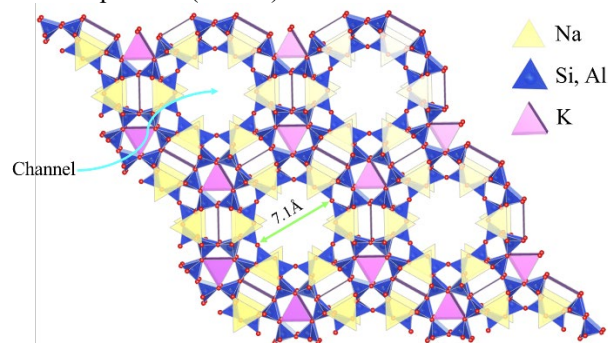


Figure 3. Crystal structure of zeolite type L (LTL). The structural tetrahedrons are composed of oxygen at the vertices and Si-Al atoms at the center. Potassium ions are part of the structure but can be exchanged for other cations.

### 3.2. Analysis by Scanning Electron Microscopy (SEM)

Figure 4 shows the SEM image where the morphology of zeolite L synthesized using mixture-2 for 90 hours can be seen. Mostly, agglomerated particles of low crystallinity (amorphous) are observed, accompanied by cylindrical shapes that are representative of zeolite type L (LTL) and that have already been reported by other authors. For example, Bhat and co-workers synthesized zeolite L using Boehmite as the aluminum source, silica in solution and KOH at a temperature of 170 °C with the simple hydrothermal treatment, to obtain nanocrystalline LTL zeolite with agglomerated particles morphology (Bhat *et al.*, 2004). However, some researchers report the existence of amorphous material mixed with crystalline structures of zeolite L (Larlus *et al.*, 2004) or the formation of amorphous material in its entirety, prior to the crystallization of zeolite L (Zhao *et al.*, 2018). The crystallization temperature in these works was around 170 °C. On the other hand, the cylindrical morphology is common in L-type zeolites and has been reported in several research works (Larlus *et al.*, 2004) (Gaona-Gómez *et al.*, 2012), (Amin *et al.*, 2018).

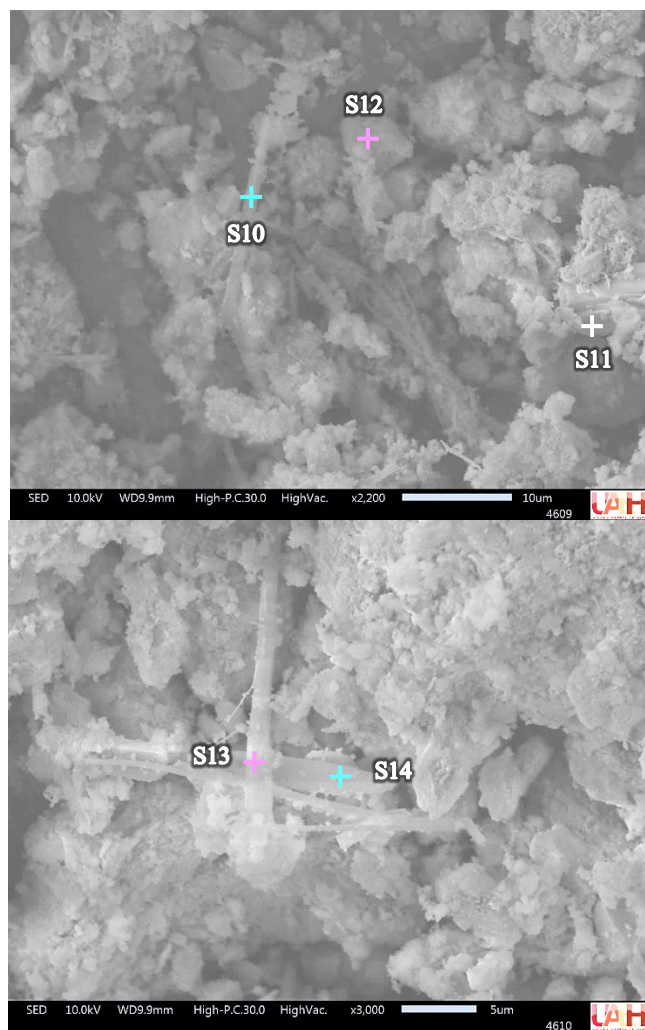


Figure 4. SEM images of zeolite L synthesized by the F-H treatment using mixture-2 for 90 hours at 145 °C. EDS microanalysis points have been marked.

taking as reference the chemical composition of zeolite L ( $K_6Na_3Al_9Si_{27}O_{72}$ ) reported by Barrer and co-workers (Barrer *et al.*, 1969).

According to the results obtained, the synthesized zeolite L has oxygen, silicon and aluminum as the most abundant elements, which are the elements that make up the structural tetrahedrons of the zeolite, see figure 3. The removable cation found in the greatest quantity is potassium because KOH was used as the main reactant. It is worth mentioning that this element can be replaced by other cations such as magnesium, calcium and copper. The potassium obtained at analysis points S10 and S12 are higher than the rest of the points, which can be attributed to residual KOH and which is part of the synthesis reagents.

Table 3: Compositional microanalysis by EDS of zeolite L (Mixture-2 at 90 hours).

Element	S10	S11	S12	S13	S14
	Atoms per unit cell				
<b>O</b>	72.0	72.0	72.0	72.0	72.0
<b>Mg</b>	0.0	1.2	0.0	0.7	0.8
<b>Al</b>	8.4	7.7	7.7	7.0	7.7
<b>Si</b>	27.6	28.3	28.3	29.0	28.3
<b>K</b>	22.5	8.1	18.5	7.9	8.9
<b>Ca</b>	1.9	2.0	3.6	3.5	2.7

### 3.3. Inductively Coupled Plasma Mass Spectrometry Analysis

The solution obtained at the end of each synthesis experiment was analyzed with the ICP technique, reporting the elemental concentrations of aluminum, potassium, sodium and silicon that are presented in Table 4. It was observed that, by increasing the initial molarity and the time of reaction, the final concentration of aluminum is higher. Regarding the concentration of potassium, it was obtained that there is a consumption of this element by increasing the reaction time. This is because the  $K^+$  ions are integrated into the structure of the synthesized zeolite (Cho *et al.*, 2017). On the other hand, the concentration of silicon and aluminum increases when using mixture-1, while with mixture-2, the concentration of silicon decreases after 50 to 90 hours of reaction time. To date, it has not been possible to accurately describe the chemical reactions that occur during the formation of zeolites (Grand *et al.*, 2016) since the crystallization process is very complex. However, it is known that  $OH^-$  ions are responsible for dissolving both silicon and aluminum and forming the new structure of the zeolite (McCormick *et al.*, 1989).

Table 3 shows the results of the semiquantitative chemical analysis by EDS, where the atoms per unit cell are calculated

Table 4: Elemental concentration in solution (mg/L) of Al, K, Na and Si at the end of the hydrothermal reaction.

Reaction conditions		Concentrations (mg/L)			
Precursor	Time (hrs)	Al	K	Na	Si
Mixture-1	50	0.2	6566.7	74.8	3199.3
	90	1.4	6500.0	70.1	3941.7
Mixture-2	50	0.5	7344.9	194.3	13445.2
	90	2.9	6747.2	165.5	12077.4

### 3.4. Exchange of zeolite L with Cu<sup>2+</sup>

The ionic exchange of the synthesized zeolites and the natural zeolite with the copper nitrate solution (Cu<sup>2+</sup>, 1000 ppm) was analyzed by means of the UV-Vis spectrophotometry method, the process for carrying out the measurements is presented in Appendix A. The concentrations of the final solution are shown in Table 5. It is observed that the adsorbed Cu<sup>2+</sup> per gram of zeolite synthesized using mixture-2 with 50 and 90 hours was 34.59 and 31.45 mg/g, respectively. These values exceed the amount adsorbed by natural zeolite, which only adsorbed 6.88 mg/g. According to the above, the ion exchange capacity of zeolite L synthesized with copper exceeds that of natural zeolite, which suggests its applicability in the area of removal of contaminants from water.

Table 5: Analysis of the ion exchange of the synthesized zeolite and the natural zeolite with a copper nitrate solution at 1000 ppm of Cu<sup>2+</sup>, at 25 °C for 24 hours.

Sample	Precursor	Reaction time (hrs)	Absorbance	Final concentration of Cu <sup>2+</sup> (ppm)	Amount adsorbed (mg of Cu <sup>2+</sup> per 1g of zeolite)
Synthesized zeolite	Mixture-1	50	0.116	607.1	<b>39.29</b>
		90	0.137	716.8	<b>28.32</b>
	Mixture-2	50	0.125	654.1	<b>34.59</b>
		90	0.131	685.5	<b>31.45</b>
Natural zeolite	....	...	0.178	931.2	6.88

## 4. Conclusions

The results of the XRD analysis showed that the synthetic zeolites obtained with reaction times of 50 and 90 hours using alkaline fusion-hydrothermal (HF) are of type L, where the level of crystallinity is relatively low.

On the other hand, the SEM images show that the morphology of the synthesized zeolite L is mostly made up of agglomerated particles and some cylindrical particles that, according to different investigations, are the most common forms to obtain the zeolite type L.

Then, the elemental composition of the solution obtained from the synthesis process of zeolite L relates to the crystallization process, since the amount of potassium in solution decreases as the reaction time elapses, due to its integration into the new crystalline structure.

The results of the exchange properties of the synthetic zeolites with Cu<sup>2+</sup> are compared with the exchange capacity of the natural zeolite. These show that the synthesized zeolites absorb a greater amount of copper ions compared to the natural zeolite. This phenomenon can be attributed to the structure of zeolite L, whose pores have a larger diameter compared to the pores of natural zeolite. Finally, the zeolite synthesized with mixture-2 for 50 hours was shown to have the best adsorptive properties, according to the results obtained by the UV-Vis spectrophotometry method. However, although the method proved to be feasible for the synthesis of zeolite L, further studies are needed to improve the synthesis conditions and increase the crystallinity of the product.

## References

- Amin, A. A., Smail, H. A., & Amin, H. I. M. (2018). Isotherm studies of adsorption of cadmium (II) ion from aqueous solution onto zeolite: Effects of time, temperature and pH. *Zanco journal of pure and applied sciences*, 30(1). doi:10.21271/zjpas.30.1.3
- Ayele, L., Pérez-Pariente, J., Chebude, Y., & Díaz, I. (2016). Conventional versus alkali fusion synthesis of zeolite A from low grade kaolin. *Applied Clay Science*, 132–133, 485–490. doi:10.1016/j.clay.2016.07.019
- Barrer, R. M., & Villiger, H. (1969). The crystal structure of the synthetic zeolite L. *Zeitschrift Fur Kristallographie. Crystalline Materials*, 128(1–6), 352–370. doi:10.1524/zkri.1969.128.16.352
- Bhat, S. D., Chaphekar, G. M., Niphadkar, P. S., Gaydhankar, T. R., Bokade, V. V., & Joshi, P. N. (2004). Dependence of synthesis parameters on physicochemical properties and catalytic performance of K-LTL zeolites. *En Studies in Surface Science and Catalysis* (pp. 233–240). Elsevier.
- Breck, D. W., & Acara, N. A. (1965). Patent Núm. 3216789
- Chen, Y., Zhang, X., Zhao, C., Yun, Y., Ren, P., Guo, W., ... Wen, X.-D. (2018). Computational insights into morphology and interface of zeolite catalysts: A case study of K-LTL zeolite with different Si/Al ratios. *The Journal of Physical Chemistry. C, Nanomaterials and Interfaces*, 122(43), 24843–24850. doi:10.1021/acs.jpcc.8b08556
- Cho, H. S., Hill, A. R., Cho, M., Miyasaka, K., Jeong, K., Anderson, M. W., Kang, J. K., & Terasaki, O. (2017). Directing the distribution of potassium cations in zeolite-LTL through crown ether addition. *Crystal Growth & Design*, 17(9), 4516–4521. https://doi.org/10.1021/acs.cgd.7b00832
- Curtis, N. J., Gascooke, J. R., Johnston, M. R., & Pring, A. (2019). A review of the classification of opal with reference to recent new localities. *Minerals (Basel, Switzerland)*, 9(5), 299. doi:10.3390/min9050299
- Database of Zeolite Structures. (s/f). Recuperado el 16 de septiembre de 2022, de Iza-structure.org website: <http://www.iza-structure.org/databases/>
- Gaona-Gómez, A., & Cheng, C.-H. (2012). Modification of zeolite L (LTL) morphology using diols, (OH)<sub>2</sub>(CH<sub>2</sub>)<sub>2n</sub>+2On (n=0, 1, and 2). *Microporous and Mesoporous Materials: The Official Journal of the International Zeolite Association*, 153, 227–235. doi:10.1016/j.micromeso.2011.12.056

- Gartzia-Rivero, L., Bañuelos, J., & López-Arbeloa, I. (2017). Photoactive nanomaterials inspired by nature: LTL zeolite doped with laser dyes as artificial light harvesting systems. *Materials*, 10(5), 495. doi:10.3390/ma10050495
- Georgieva, V., Retoux, R., Ruau, V., Valtchev, V., & Mintova, S. (2018). Detection of CO<sub>2</sub> and O<sub>2</sub> by iron loaded LTL zeolite films. *Frontiers of Chemical Science and Engineering*, 12(1), 94–102. doi:10.1007/s11705-017-1692-5
- Gomez, A. G., de Silveira, G., Doan, H., & Cheng, C.-H. (2011). A facile method to tune zeolite L crystals with low aspect ratio. *Chemical Communications (Cambridge, England)*, 47(20), 5876–5878. doi:10.1039/c1cc10894h
- Gottardi, G., & Galli, E. (2013). *Natural Zeolites*. Berlin, Alemania: Springer.
- Guth, J.-L., & Kessler, H. (1999). Synthesis of aluminosilicate zeolites and related silica-based materials. En *Catalysis and Zeolites* (pp. 1–52). Berlin, Heidelberg: Springer Berlin Heidelberg.
- Insuwan, W., Jungsuttiwong, S., & Rangsriwatananon, K. (2015). Host-guest composite materials of dyes loaded zeolite LTL for antenna applications. *Journal of luminescence*, 161, 31–36. doi:10.1016/j.jlum.2014.12.031
- Itani, L., Bozhilov, K. N., Clet, G., Delmotte, L., & Valtchev, V. (2011). Factors that control zeolite L crystal size. *Chemistry (Weinheim and Der Bergstrasse, Germany)*, 17(7), 2199–2210. doi:10.1002/chem.201002622
- Larus, O., & Valtchev, V. P. (2004). Crystal morphology control of LTL-type zeolite crystals. *Chemistry of Materials: A Publication of the American Chemical Society*, 16(17), 3381–3389. doi:10.1021/cm0498741
- Lee, Y.-J., Lee, J. S., & Yoon, K. B. (2005). Synthesis of long zeolite-L crystals with flat facets. *Microporous and Mesoporous Materials: The Official Journal of the International Zeolite Association*, 80(1–3), 237–246. doi:10.1016/j.micromeso.2004.12.003
- McCormick, A. v., & Bell, A. T. (1989). The solution chemistry of zeolite precursors. *Catalysis reviews, science and engineering*, 31(1–2), 97–127. doi:10.1080/01614948909351349
- Pérez González, N. K. (2019). *Síntesis y Caracterización de Zeolitas a Partir de Clinoptilolita Natural y Desechos de Aluminio*. Universidad Autónoma del Estado de Hidalgo, Mineral de la Reforma, Hidalgo, México.
- Sato, M., Morikawa, K., & Kurosawa, S. (1990). X-ray Rietveld analysis of cation exchanged zeolite-L(LTL). *European journal of mineralogy*, 2(6), 851–860. doi:10.1127/ejm/2/6/0851
- Veiga-Gutiérrez, M., Woerdemann, M., Prasetyanto, E., Denz, C., & De Cola, L. (2012). Assembly: Optical-tweezers assembly-line for the construction of complex functional zeolite L structures (adv. Mater. 38/2012). *Advanced Materials (Deerfield Beach, Fla.)*, 24(38), 5198–5198. doi:10.1002/adma.201290230
- Zhang, F., Luo, Y., Chen, L., Chen, W., Hu, Y., Chen, G., Song, W. (2020). Designer synthesis of ultra-fine Fe-LTL zeolite nanocrystals. *Crystals*, 10(9), 813. doi:10.3390/cryst10090813
- Zhao, C., Wu, B., Tao, Z., Li, K., Li, T., Gao, X., Li, Y. (2018). Synthesis of nano-sized LTL zeolite by addition of a Ba precursor with superior n-octane aromatization performance. *Catalysis science & technology*, 8(11), 2860–2869. doi:10.1039/c8cy00661j

## Appendix A. Measurement of Cu<sup>2+</sup> concentration by UV-VIS spectrophotometry.

The detection of copper levels in solution (ppm) was carried out using a spectrophotometer (Thermo Scientific GENESYS 10S), taking as reference the calibration points of 0, 500, 1000,

1500, 2000 and 2500 ppm of Cu<sup>2+</sup> made from a solution of Cu(NO<sub>3</sub>)<sub>2</sub>·3H<sub>2</sub>O. Initially, a scan of each calibration point was performed, finding that the highest absorbance is at 808 nm, as can be seen in Figure 5. . Subsequently, the absorbance-concentration calibration curve was plotted, using the wavelength of 808 nm. Figure 6 shows the linear fit and its equation.

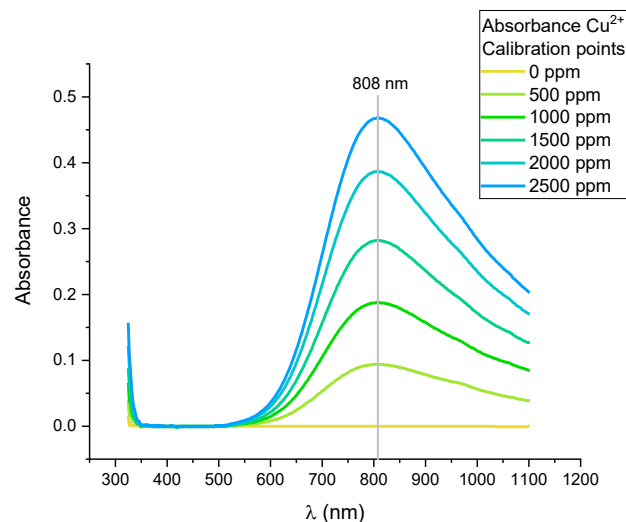


Figure 5. Absorbance of the copper nitrate calibration points. Scanning from 325-1100 nm.

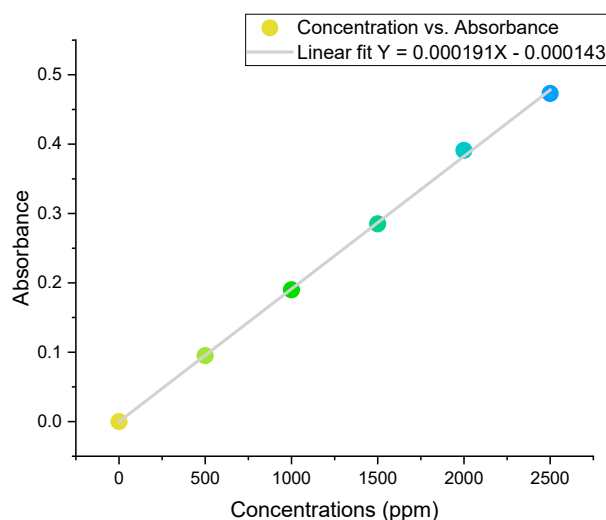


Figure 6. Calibration curve for detection of Cu<sup>2+</sup>. The absorbance of the different calibration points (0-500 ppm) was measured using a wavelength of 808 nm.